Fuzzy ARTMAP Neural Networks for Automatic Feature Extraction from Aerial Images and Lidar Data

M. SALAH, J. C. TRINDER

School of Surveying and Spatial Information Systems, The University of New South Wales, Sydney, 2052 Australia
Telephone: (+61 2 938 54197)
Fax: (+ 61 2 9313 7493)
Email: (m.gomah; j.trinder)@unsw.edu.au

1. Introduction

In this paper we applied the fuzzy ARTMAP algorithm for combining multispectral aerial imagery and lidar data so that the individual strengths of each data source can compensate for the weakness of the other. Test data from four different study areas with different characteristics have been used. First, we filtered the lidar point clouds to generate a Digital Terrain Model (DTM), and then the Digital Surface Model (DSM) and the Normalized Digital Surface Model (nDSM) were generated. After that, we have derived 22 attributes from both aerial image and lidar data by a number of algorithms. The attributes include those derived from the Grey Level Co-occurrence Matrix (GLCM), Normalized Difference Vegetation Indices (NDVI) and slope. Finally, a Fuzzy ARTMAP was used to detect buildings, trees, roads and grass from the aerial image, lidar data and the generated attributes.

The rules for tuning the parameters of the Fuzzy ARTMAP and its relation to the produced classification accuracy have been studied. The ability of the Fuzzy ARTMAP to detect features has been evaluated and compared against other classifiers. Also, the transferability of information from one data set to another has been tested. Finally, the contributions of the individual attributes to the quality of the classification results were assessed.

2. Previous work

The numbers of studies that have utilized Fuzzy ARTMAP for highly spectrally dimensional image analysis are limited. Carpenter et al. (1995) have developed a new methodology for automatic mapping of vegetation from Landsat Thematic Mapper (TM) and terrain data, based on the fuzzy ARTMAP neural networks. Mannan et al. (1998) have applied the fuzzy ARTMAP to the supervised classification of multi-spectral remotely-sensed images obtained from the LISS-II sensor of the Indian IRS-1B satellite. Recently, Gamba and Houshmand (2001) have discussed the segmentation of urban optical and SAR images by means of competitive neural networks based on Adaptive Resonance Theory (ART).

3. Study area and data sources

Four test data sets of different characteristics and different sizes were used in this study as shown and summarized in fig. 1 and table 1 respectively.

Test area	Size	Lidar Data		Aerial images	
		Sensor	wavelength	bands	pixel size
UNSW	0.5 x 0.5Km	Optech ALTM 1225	1.047µm	RGB	10cm
Bathurst	1 x 1Km	Leica ALS50	1.064µm	RGB	50cm
Fairfield	2 x 2Km	Optech ALTM 3025	1.047µm	RGB	15cm
Memmingen	2 x 2Km	TopoSys	1.56µm	CIR	50cm

Table 1. Characteristics of image and lidar data sets.

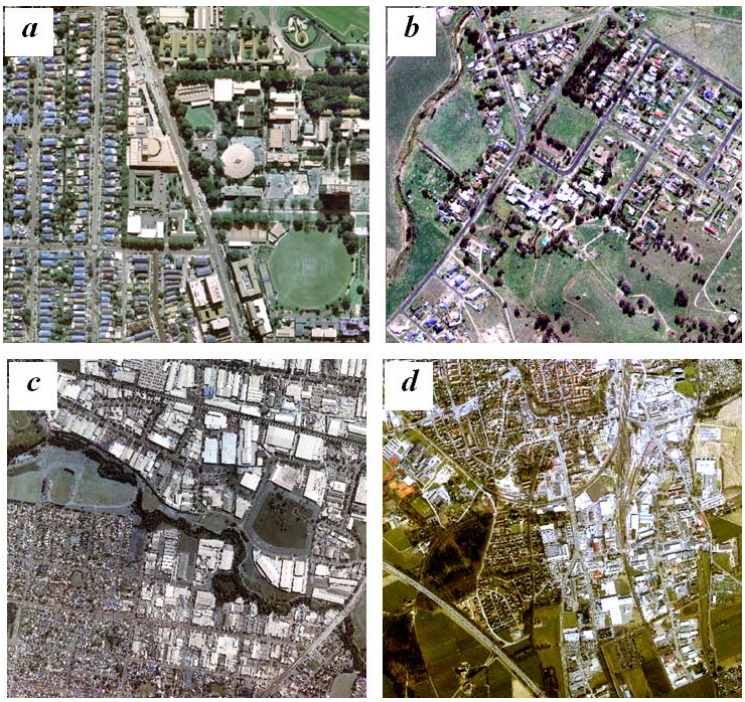

Figure 1. Orthophotos for: *(a)* UNSW; *(b)* Bathurst; *(c)* Fairfield; and *(d)* Memmingen.

4. Filtering of lidar point clouds

Filtering is the process of separating on-terrain points from points falling onto natural and human made objects. A filtering technique based on a linear first-order equation which describes a tilted plane surface has been used (Salah et al. 2009). After that, the filtered lidar points were converted into an image DTM, the DSM was generated from the original Lidar point clouds and the nDSM was generated by subtracting the DTM from the DSM. Fig. 2 shows the results for the UNSW test area.

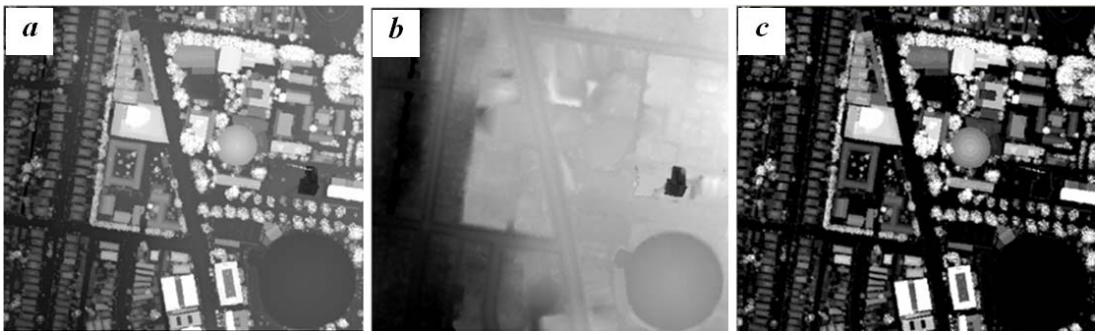

Figure 2. *(a)* DSM, *(b)* DTM and *(c)* the nDSM.

5. Generation of attributes

Features or attributes calculated for pixels are presented as input data for a classification method. In our test, a set of 78 possible attributes were selected. Because of the way the texture equations derived from the GLCM are constructed, many of them are strongly correlated with one another. Based on these facts, only 22 of the 78 possible attributes were uncorrelated and hence available for the classification process as shown in table 2. Fig. 3 (a - f) shows the generated attributes from the nDSM plus the generated NDVI.

Attributes	Attribute	R	G	B	I	DSM	nDSM
Spectral	Mean	▨	▨	▨	▨	▨	▨
	St. Deviation	▨	▨	▨	▨	▨	▨
	Strength	▩	▩	▩	▩	▩	▩
GLCM	Contrast	▨	▨	▨	▨	▨	▨
	Dissimilarity	▨	▨	▨	▨	▨	▨
	Homogeneity	▩	▩	▩	▩	▩	▩
	A.S.M	▨	▨	▨	▨	▨	▨
	Entropy	▩	▩	▩	▩	▩	▩
	Mean	▨	▨	▨	▨	▨	▨
	Variance	▨	▨	▨	▨	▨	▨
	Correlation	▨	▨	▨	▨	▨	▨
Height	SD	▨	▨	▨	▨	▩	▩
	Slope	▨	▨	▨	▨	▩	▩

Table 2. ▨ The full set of the attributes; ▩ attributes available for the classification.

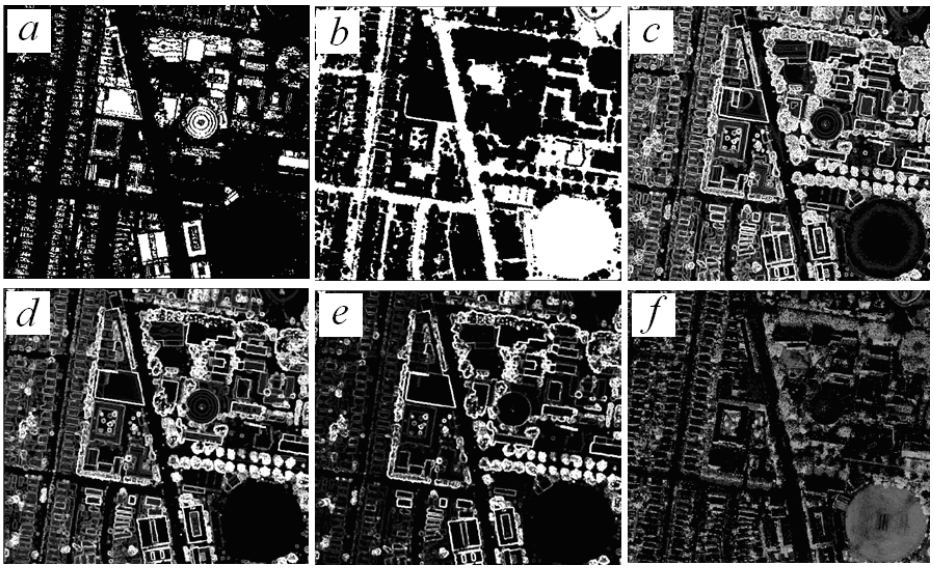

Figure 3. *(a)* GLCM-homogeneity of the nDSM, *(b)* GLCM-entropy of the nDSM, *(c)* Slope percent of the nDSM, *(d)* SD of the nDSM, *(e)* Texture strength of the nDSM, *(f)* The NDVI.

6. Fuzzy ARTMAP classification

Fuzzy ARTMAP is one of the most commonly used neural network classifiers. It performs classification of remotely sensed imagery through Adaptive Resonance Theory (ART) based neural network analysis (Grossberg 1976). Compared to traditional classifiers, it is faster and has a smaller number of parameters to manage (Mannan et al. 1998). Fig. 4 shows the architecture of the Fuzzy ARTMAP. A detailed description is given by Carpenter et al. (1991).

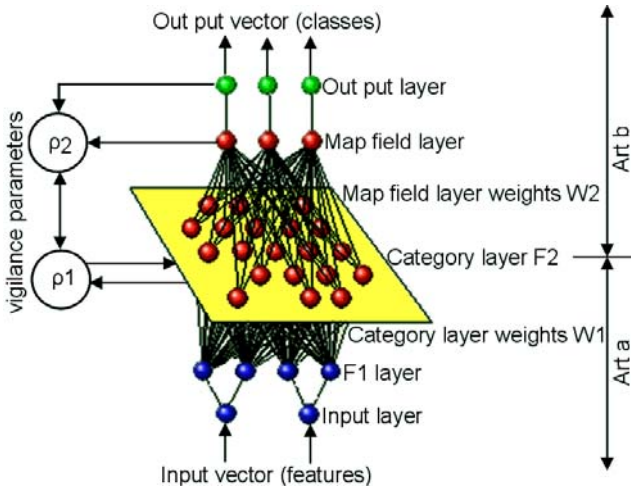

Figure 4. Fuzzy ARTMAP architecture.

For our case, the Fuzzy ARTMAP has 29 input neurons which are: 22 generated attributes, 3 image bands (R, G and B), intensity image, DTM, DSM and nDSM. First, a total of twenty samples evenly distributed through the image were selected as training data for each class. Table 3 summarizes the Fuzzy ARTMAP architectures for the classification of the four test areas and fig. 5 shows the classification results.

	F1 (input layer)	F2 (category layer)	Iterations	Weights
UNSW	29	1494	3433	Initially set to 1
Bathurst	29	1915	4025	
Fairfield	29	2171	46674	
Memmingen	29	3357	17688	

Table 3. Fuzzy ARTMAP architectures for the four test areas.

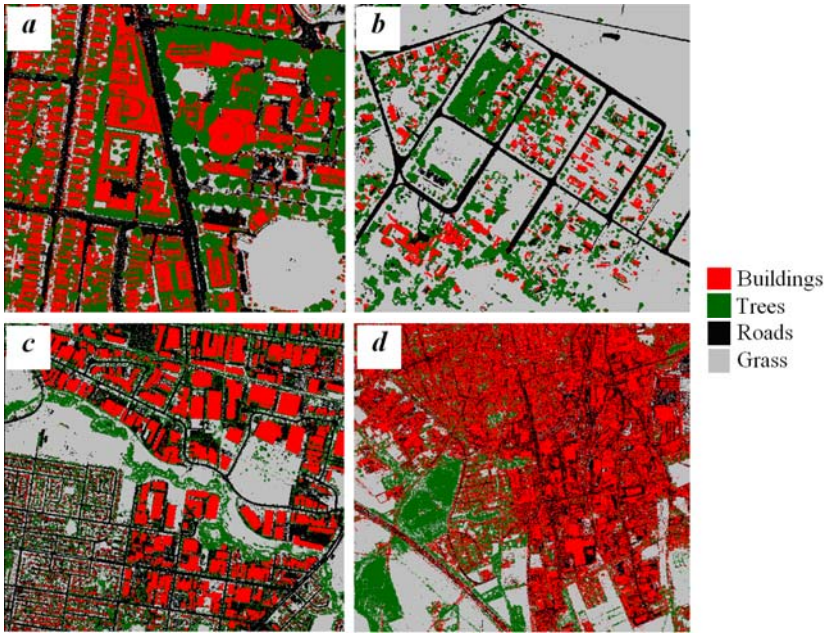

Figure 5. Classification results using the fuzzy ARTMAP for: *(a)* UNSW; and *(b)* Bathurst; *(c)* Fairfield; and *(d)* Memmingen.

7. Testing the performance of Fuzzy ARTMAP parameters

Five parameters should be specified for the Fuzzy ARTMAP: the Choice parameter α (a small positive constant); two learning parameters β_1 and β_2 ($0 \leq \beta \leq 1$); and two vigilance parameters ρ_1 and ρ_2 (normally set very close to 1). In order to study the relation between the produced classification accuracy and the ARTMAP parameters, first, we specified the ARTMAP parameters as shown in table 4. After that, each parameter was changed gradually and the classification accuracies were computed and plotted against the parameter value as shown in fig. 6.

Parameter	α	β_1	ρ_1	β_2	ρ_2
Value	0.01	1	0.98	1	1

Table 4. The chosen parameters for the training of fuzzy ARTMAP

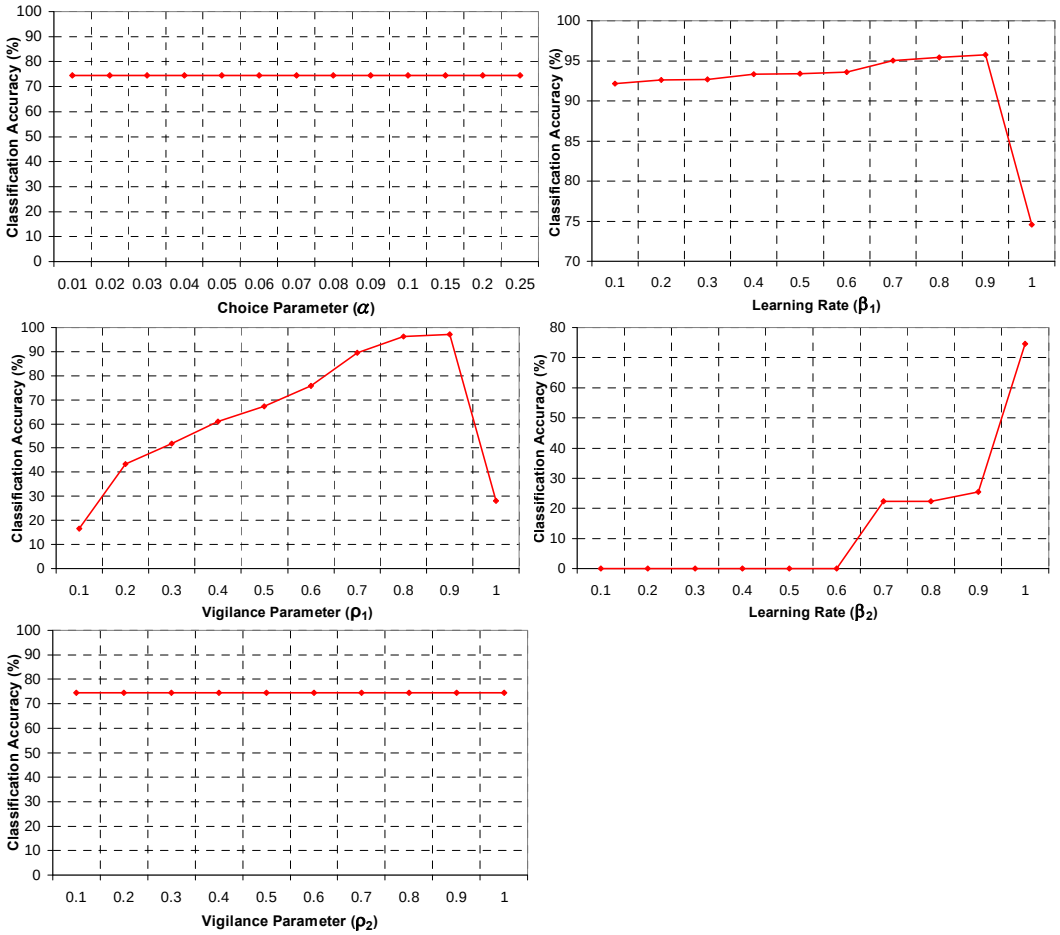

Figure 6. The relation between the Fuzzy ARTMAP parameters and the produced classification accuracy.

8. Fuzzy ARTMAP against other classifiers

To evaluate the ability of the Fuzzy ARTMAP to detect features, the Fuzzy ARTMAP has been compared against two classifiers of different characteristics (the Self Organizing Map (SOM) and the Classification Trees (CT)) as shown in fig. 7. The results show that the Fuzzy ARTMAP has performed the best followed by SOM and CT. The produced classification accuracies were over 95% except for Memmingen test area, over 88%, which has quite different sensors and scene characteristics, see table 1.

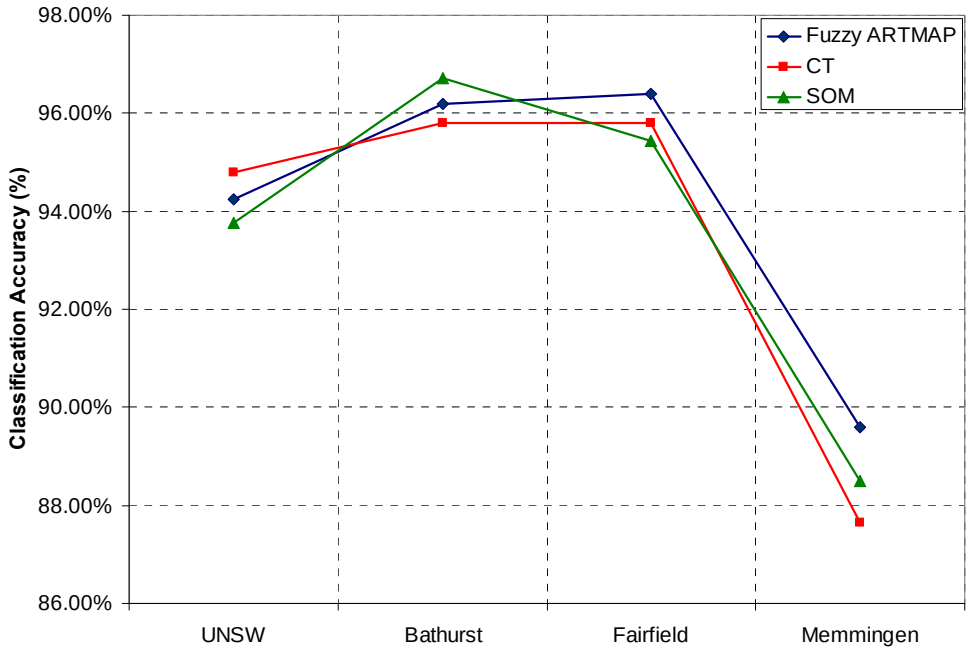

Figure 7. Fuzzy ARTMAP against RT and SOM.

9. Transferability of information from one data set to another

In order to test how well the information is transferable from one data set to another, instead of training the network for each individual case, the weights derived for the UNSW test area have been used to classify the other three test areas; fig. 8 shows the produced classification accuracies. For Memmingen Test area, the UNSW weights resulted in very poor classification accuracy since both data sets have different ground cover types and different lidar and aerial image characteristics as mentioned in table 1.

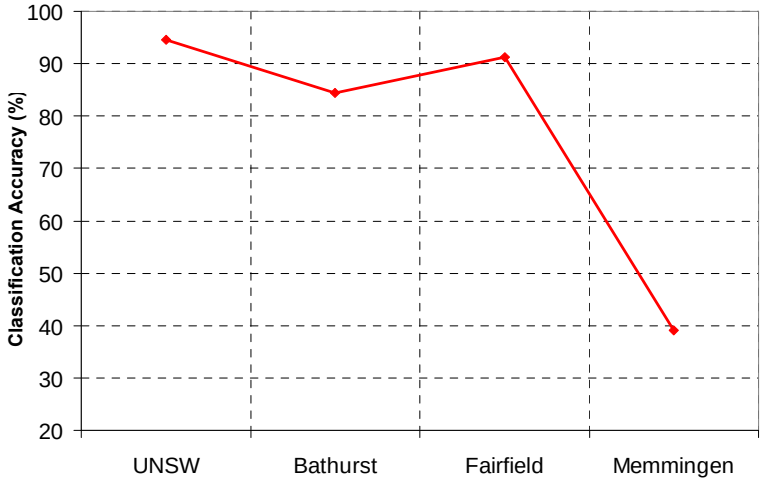

Figure 8. The performance when the weights derived for UNSW data set were used to classify the other three data sets.

10. Contributions of the individual attributes

Furthermore, the contributions of the individual attributes to the quality of the classification results were evaluated. Fig. 9 shows the improvement in the average classification accuracy by each individual attribute.

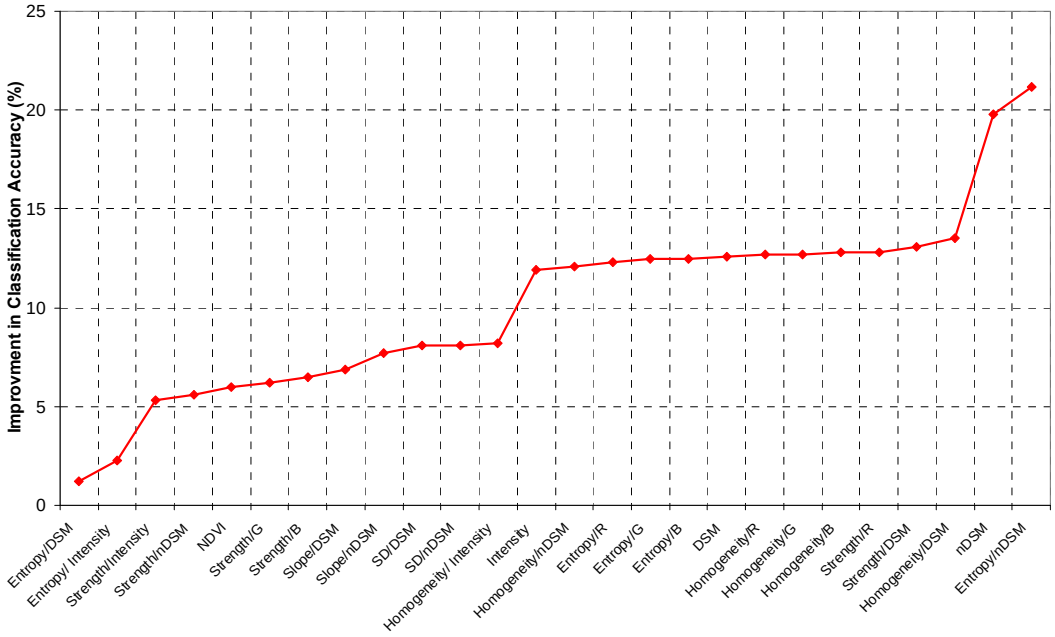

Figure 9. Contributions of the individual attributes to the quality of the classification.

11. Conclusion

The Fuzzy ARTMAP has been successfully applied for image and lidar data fusion. The results highly recommend setting the vigilance parameter ($\rho 1$) and the learning rate ($\beta 1$) very close to one but not equal to one. The results also showed that the weights generated for one test area can be used to classify other areas with similar ground cover types and for lidar and aerial image data with similar characteristics. Finally, the nDSM and entropy from the nDSM performed the best, improving the average accuracy by 19.8 and 21.2%, respectively.

12. Acknowledgements

The authors wish to acknowledge AAMHatch for the provision of the UNSW and Fairfield datasets, the Department of Lands, NSW, Australia for Bathurst data sets and the TopoSys GmbH, Germany for the Memmingen datasets.

13. References

Carpenter G. A., Crossberg S. and Reynolds J. H., 1991, ARTMAP: supervised real time learning and classification of nonstationary data by a self-organizing neural network. *Neural Networks*, 4: 565-588.

Carpenter G., Gjaja M., Gopal S. and Woodcock C., 1995, ART neural networks for remote sensing: vegetation classification from Landsat TM and terrain data, *IEEE Transactions on Geoscience and Remote Sensing*, 35: 308-325.

Gamba P. and Houshmand B., 2001, An efficient neural classification chain of SAR and optical urban images. *International Journal of Remote Sensing*, 22(8): 1535-1553.

Grossberg S., 1976, Adaptive pattern classification and universal recording I: parallel development and coding neural feature detectors. *Biological Cybernetics*, 23, 121: 134.

Mannan B., Roy J. and Ray A. K., 1998, Fuzzy ARTMAP supervised classification of multi-spectral remotely-sensed images. *International Journal of Remote Sensing*, 19(4):767-774.

Salah M., Trinder J. and Shaker A., 2009, Evaluation of the self-organizing map classifier for building detection from lidar data and multispectral aerial images. *Journal of Spatial Science*, accepted.